NANOPHAGE FOR SELECTIVE KILLING OF MULTI-DRUG RESISTANT BACTERIA

By

FARZANA NUSHIN REZVI

A thesis submitted to the

School of Graduate Studies

Rutgers, The State University of New Jersey

In partial fulfillment of the requirements

For the degree of

Master of Science

Graduate Program in Chemistry and Chemical Biology

Written under the direction of

Dr Ki Bum Lee

And approved by

_____

_____

_____

New Brunswick, New Jersey

October, 2018

ABSTRACT OF THE THESIS

NANOPHAGE FOR SELECTIVE KILLING OF MULTI-DRUG RESISTANT BACTERIA

by FARZANA NUSHIN REZVI

Thesis Director: Professor Ki-Bum Lee

In light of concerns in recent years of the emergence of antibiotic resistance in pathogenic bacteria, this project involves developing a novel kind of nanoparticle for targeting and killing multi drug resistant E. coli. In this approach, we combine the essence of two well researched fields – nanoparticle and bacteriophage therapy to develop a novel nanoparticle. The protein that helps the bacteriophage M13 infect E. coli is identified, isolated, and conjugated on the surface of a mesoporous silica nanoparticle bearing a magnetic core. The mesoporous silica shell can be packed with ROS generators like porphyrin; and the resulting nanoparticle (aptly termed 'NanoPhage' has the ability to selectively target and kill E. coli when subjected to magnetic hyperthermia and photodynamic therapy. Multiple drug resistant *Escherichia coli* BL21DE3 are treated with NanoPhage and the temperature is raised to 42 °C and 48 °C (individually) to show significant bacterial killing efficiency. The bacteria survival rate after 24 hours can be down to as low as 10% after simultaneous therapy of hyperthermia and photodynamic therapy after 30 minutes of treatment, owing to denaturation of proteins in the cell body and the cell membrane of E. coli, and ROS generation by porphyrin – that oxidizes the membrane-associated complexes of bacteria. These results indicate that NanoPhage-based physical treatment can be an alternative strategy to kill bacteria without acquiring antibiotic resistance and can be used for many purposes - thus inspiring therapeutic and environmental applications.

Acknowledgements

First and foremost, I would like to express my profound gratitude to my advisor, Professor Dr. KiBum Lee, who gave me an opportunity to work in his lab for my masters' degree. He is an exceptional mentor who inspired, encouraged and supported me with his positive energy and suitable advice whenever I encountered scientific and personal difficulties. Without his support, it would have been highly unlikely for me to come this far in my career.

I also would like to extend my gratitude to my other committee members, Professor Dr. Ralf Warmuth and Professor Dr. Wilma Olson for their critical comments and valuable suggestions on my thesis. Their comments and suggestions have contributed to my understanding of the subject matter much better and have helped me successfully conclude my masters' degree.

Next, I would like to express my sincere and profound gratitude to the post-doctoral candidate, Dr. Hyeonryeol Cho under whose direct supervision I worked in this project. His depth of knowledge, sense of perfection and work ethic contributed greatly to my learning experience as a graduate student. It would have been impossible for me to successfully finish this my degree without his guidance and support. He has invested a significant part of his post-doctoral time to train me and take care of me in every conceivable way. I also have learned a lot of from him on how to do good research and be a hardworking and creative scientist. He has several qualities that I would like to emulate in my future scientific career.

All the KBLEE group members played very essential roles during my life as a masters' student at Rutgers. They have all contributed to making my life here very

enjoyable and full of wonderful experiences. From the very beginning, Thanapat Pongkulapa (Top) has always been there to help me by lending books, teaching various techniques and giving me tips and advice whenever needed. I feel very thankful to have come in the acquaintance of such a nice, sweet and generous person like him. Next, I would like to credit Hudifah Rabie for being an active part of our project by being responsible for synthesizing nanoparticles; Yixiao Zhang for acting as a true 'older brother' figure by lifting my spirits and encouraging me every step along the way. Other members of Subgroup C (Skylar Cheung, Brian Conley and Jin Ha Choi) and other lab members, namely Chris Rathnam, Letao Yang, Shenqiang Wang (Jason) and Jeffery Luo for providing useful feedback regarding the progress of my project and ways to improve in our biweekly and group meetings. I would like to give special thanks to St. Dean Chueng for his IT and lab management expertise and for having patience to answer all my (even irrelevant) questions. The two years that I have worked in the lab in the proximity of all these hard working and creative individuals, have contributed massively to my personal and academic growth. I also would also like to extend my special thanks to undergraduate students in the lab, Cara Wong and Brianna Berlin for their company, and for all the girl talk, gossips and laughs that we shared.

Each person working in the lab has unique skills and almost all of them have been ready to extend a helping hand whenever needed. Among much others, the lab has taught me the importance of cooperation and efficient communication in a research environment. The lab members had started feeling like my family. The alumni meetings (and talks) have helped me develop a perspective on life after graduation and have inspired me do things I didn't think I could do. I will cherish the connections that I have made in the lab for years to come.

Finally, I would like to express my deepest gratitude to my family. My parents' hard work and financial and emotional investment on me allowed me to have many wonderful opportunities in life. I can never thank them enough for their dedication in raising us as educated and humane individuals, and for their words of support whenever I needed them most. They helped me develop a positive attitude of life by not losing faith in me, especially when the future looked grim. My older brother (who I call Bhaiya) always stated distinctly that he expects nothing less than the best from me. I am here today because of them, and no words will be enough to express the extent of gratitude I feel, but I hope they will know how much I love, and am grateful to, them.

Dedication

To those who helped me seek a light in me

When I could not find one in myself

I will always remain thankful to you more than words can express.

Table of Contents

List of Figures

Chapter 1

Introduction

Antibiotic resistance is an increasing trend among pathogenic bacteria, thus posing a severe threat to human health and well-being[1,2] worldwide. The emergence of antibiotic resistant strains of bacteria is an inevitable phenomenon as it is a result of evolutionary selection[3] that selects for genes conferring competing characteristics that arise by mutation in each successive generation and has perennially been taking place in bacterial populations; and since bacteria asexually reproduce at logarithmic rates, it is possible to have the resistance gene transmitted to the majority of bacterial strain. However, in more recent years the excessive use (and abuse) of antibiotics[4] at low concentrations[5] in food, livestock[4], hospitals and communities (for the purposes of water disinfection, medicine, food packaging, textile industry, etc.) along with over-necessary prescribing of antibiotics by medical professionals[6] has expedited the emergence of multiple drug resistant bacteria (MDRB)[3,7]. The horizontal transfer of antibiotic resistance genes among microbial populations[8] further exacerbates the problem[2,7]. The widespread distribution of antibiotic-resistant genes (that render antibiotic drugs harmless to the bacteria) has made infectious diseases that were once easily treatable - deadly again[1,9,10]. An increase in multiple drug resistant bacteria (which are informally known as superbugs) population is therefore a severe threat to human health in the future that necessitates the need to develop alternative means to kill bacteria without the use of traditional antibiotics. For diseases caused by Gram-negative bacteria, resistant bacteria are even a bigger problem as the pipeline for the development of new antimicrobials that target Gram-negative bacteria remains empty[11], largely due to the presence of an outer membrane that serves as a highly impermeable barrier, thereby acting as a defense

mechanism. As the rate of development of novel antibiotics has declined, alternatives to antibiotics are beginning to be considered in both animal agriculture and human medicine. These non-antibiotic approaches include phage therapy, phage lysins, bacteriocins, and predatory bacteria[12], and nanoparticles[13].

Several classes of antibacterial nanoparticles and nanosized carriers have proven their effectiveness for treating bacterial infections, including antibiotic-resistant ones, in experimental models and *in vivo*[13]. Nanoparticles offer improved antibacterial properties compared to organic antibacterial drugs principally due to their high surface area to volume ratio, that results in appearance of novel mechanical, electrical, chemical, optical, magnetic, magneto-optical, and electro-optical properties of the nanoparticles that are different from their bulk properties[14]. The mechanisms of nanoparticle toxicity depend on composition, surface modification, intrinsic properties, and the bacterial species.[15-17]. Nanoparticle toxicity is generally believed to be triggered by the induction of oxidative stress by free radical formation[15] (i.e., ROS generation) but the mechanisms are very complex and depends on the physicochemical properties of the nanoparticles[15]. TiO_2 and ZnO nanopaticles are known to have mutagenic potential that brings about frameshift mutation in *Salmonella typhimurium* (–)[18]. Metallic and ionic forms of copper in Cu based nanoparticles produce hydroxyl radicals that damage DNA and essential proteins of the bacterial cell [19]. Ag nanopartcles modified with titanium compounds that are toxic to E. coli and S. aureus, by naturally interacting with the membrane of bacteria and disrupting the membrane integrity, and moreover binding to sulfur, oxygen, and nitrogen atoms of essential biological molecules and thereby inhibiting bacterial growth[20]. NO nanoparticles are able to cause structural change in the bacterial membrane and produce reactive nitrogen species (RNS), which cause modification of essential proteins of bacteria[21]. However, concerns have been raised on the

effects of metal nanoparticle persistence and toxicity effects on the beneficial microbes, microbial communities in ecosystems, and public health[22]. For example, exposure to soluble Ag compounds is known to produce toxic effects like eye, skin, respiratory, and intestinal tract irritations; liver and kidney damage; and unwarranted changes in blood cells[23]. In addition, adverse toxic effects have also been reported due to prolonged exposure to some nanoparticles therapy[16,24].

The specific killing of bacterial cells has also been accomplished using bacteriophages. Bacteriophages are infectious viruses that have a natural tendency to attack specifically target, and kill bacteria during its own reproductive life cycle[25-27] by injecting its own DNA, a feature that can be manipulated and used for targeted bacterial killing (phage therapy)[27-30]. Using bacteriophages as therapeutic agents present a number of advantages; such as the phages being very specific (thus avoiding the chances of developing secondary infections)[28,31], and that side effects have not been reported (in contrast to traditional antibiotics, for which side effects are common). However, compared to nanoparticles, bacteriophages also present disadvantages in that they are very specific and are difficult to be functionalized, have low stability (less shelf life), and can only be taken intravenously[32]. There may also be unknown consequences of introducing a biological sample (with its own DNA) to interact with bacterial cells inside the human body. In contrast, unlike biological specimen, nanoparticles can be manufactured and stored for a long time and in many different solvents[33], can be modified (on the surface and intrinsically) in ways to make it more suitable for bacteria killing, like ROS generation, hyperthermia, drug loading capacity, etc[33]. They can also be administered in more feasible routes (orally or inhaled), instead of only having to rely only on intravenous injection[33] (unlike bacteriophage treatment).

For this research project, we use a novel concept that combines the 'art' of bacteriophage therapy with nanoparticles by enabling the nanoparticle to interact closely with the bacterial cell body. We do this by manipulating the protein of the bacteriophage that helps it penetrate into the bacterial cell membrane, by identifying and isolating it and then conjugating it on the nanoparticle surface. This is a unique approach to bacteria killing, as no nanoparticles have been developed that is able to use a bacteriophage protein for penetration of cell membrane. To achieve this bacteriocidal effect, our nanoparticle (synthesized as mesoporous silica nanoparticles with a magnetic core) are coated with g3p proteins, which are minor coat proteins derived from the bacteriophage[34] M13 that is known to infect Escherichia coli (E. coli). g3p is found on one tip of the filamentous phage [34,35], and is known to be involved in the infection of E. coli cells carrying F-pili[35] by mediating penetration of the phage into the host (E. coli) cytoplasm. The core of the nanoparticle contains zinc doped iron oxide ($ZnFe_2O_4$) that makes it susceptible to magnetic hyperthermia. Hyperthermia involves raising the temperature of local environment of a cell, using magnetic nanoparticles subjected to high frequency magnetic field[36], and heating the cells indirectly in changing the physiology of targeted cells finally leading to cell death[37] Hyperthermia has been studied for a long time as a cell killing method and has been widely suggested as a method for treating cancer - complementing radio and chemotherapy. Hyperthermia treatment can be classified into distinct types depending on the degree of temperature rise. Cells subjected to hyperthermia heated upto high temperatures of >46 °C (up to 56°C) which causes cells to undergo protein denaturation, coagulation, carbonization or direct tissue necrosis[38]. The efficiency of any hyperthermia treatment critically depends on the temperatures generated near the nanoparticle, duration of exposure etc[39].

In order to improve efficiency of killing, the nanoparticles are also 'packed' with porphyrin derivatives. Porphyrins are very efficient water-soluble conjugated aromatic dyes that have

previously been reported to be used in selective cell killing[40], and are naturally found in the hemoglobin of human blood cells. Porphyrin derivatives have the potential to be used in photodynamic therapy and have a high propensity to accumulate in the membranes of intracellular organelles that are necessary for cell survival, (like lysosomes and mitochondria). When exposed to light of a specific frequency, porphyrins are able to highly reactive oxygen species[41] (ROS), usually singlet oxygen, as well as superoxide anion, free hydroxyl radical, or hydrogen peroxide, that helps to kill cells by oxidizing the cellular membranes. Along with hyperthermia treatment, ROS generation by porphyrin is expected to improve selective cell killing by the NanoPhage. Since porphyrins are light sensitive, using porphyrin derivatives also help to track the NanoPhage particles during treatment with bacteria.

Chapter 2:

Results and Discussion:

2.1 Size of magnetic core in silica nanoparticles

For the specific targeting of bacteria using MCNP, a zinc doped iron oxide core ($ZnFe_2O_4$) was developed, which was later coated with a mesoporous silica shell. The ferromagnetism of iron oxide decreases dramatically when the core size is below the critical diameter (critical diameter for iron oxide is 128 nm) but magnetization can be greatly improved by doping with a divalent metal ion[42]. Zn is one of the most commonly used elements to dope into Fe_3O_4[43,44].

The factors that affect heating efficiency of magnetic nanoparticles by magnetic hyperthermia, and the phenomenon of heat generation of MCNPs have been studied extensively, with an aim to develop MCNPs for maximum heat generation[36].

Heat generation in superparamagnetic MNPs occurs by two main mechanisms : Brownian relaxation (occurs by nanoparticle rotation leading to the motion of MNPs against the viscous forces in the fluid dispersion) and Neel relaxation (occurs due to re-orientation of the magnetic moment inside the MNP in response to the alternating magnetic field), as described by the linear response theory (LRT)[45,46]. LRT has been used to theoretically calculate the amount of heat generated by MCNPs, and based on this theory, among many other factors, the size of MCNP plays a major influence in the heat generation capacity of nanoparticles[36].

Based on this theory, we tested our nanoparticles with differently sized magnetic cores. The three different sizes of cores available in our lab were 5 nm, 10 nm and 20 nm. Since the

surface temperature of the cores (and thereby, nanoparticles) is very important in bacterial killing efficiency, it is important that we select a core with the greatest heating efficiency.

The three kinds of magnetic cores were subjected to hyperthermia treatment, using the same settings, and allowed to heat up until a constant temperature was reached. The following diagram illustrates how a sample is placed inside a hyperthermia coil.

Figure 1: How a sample is placed inside a magnetic hyperthermia coil.

As can be seen from the setting of the tube in the coil, there is significant chance of heat loss when we subject a sample to hyperthermia. As MCNPs compose a very small part of the LB broth in the suspension the temperature rise of the LB broth will be less compared to the surface temperature of MCNP. Therefore, the registered temperature of the aqueous LB broth in which the bacterial cells are suspended is likely to be different from the surface temperature of the MCNPs. But the sample used was insulated as best as possible to minimize heat loss. Instead of using water as the solvent to suspend the magnetic cores, olive oil was used for its relatively low specific heat capacity, as the temperature rise of the olive oil is more responsive to the heat energy generated on the surface of magnetic cores by hyperthermia (if water or any other aqueous solution was used, much of the heat generated would be lost to the environment before causing a temperature rise).

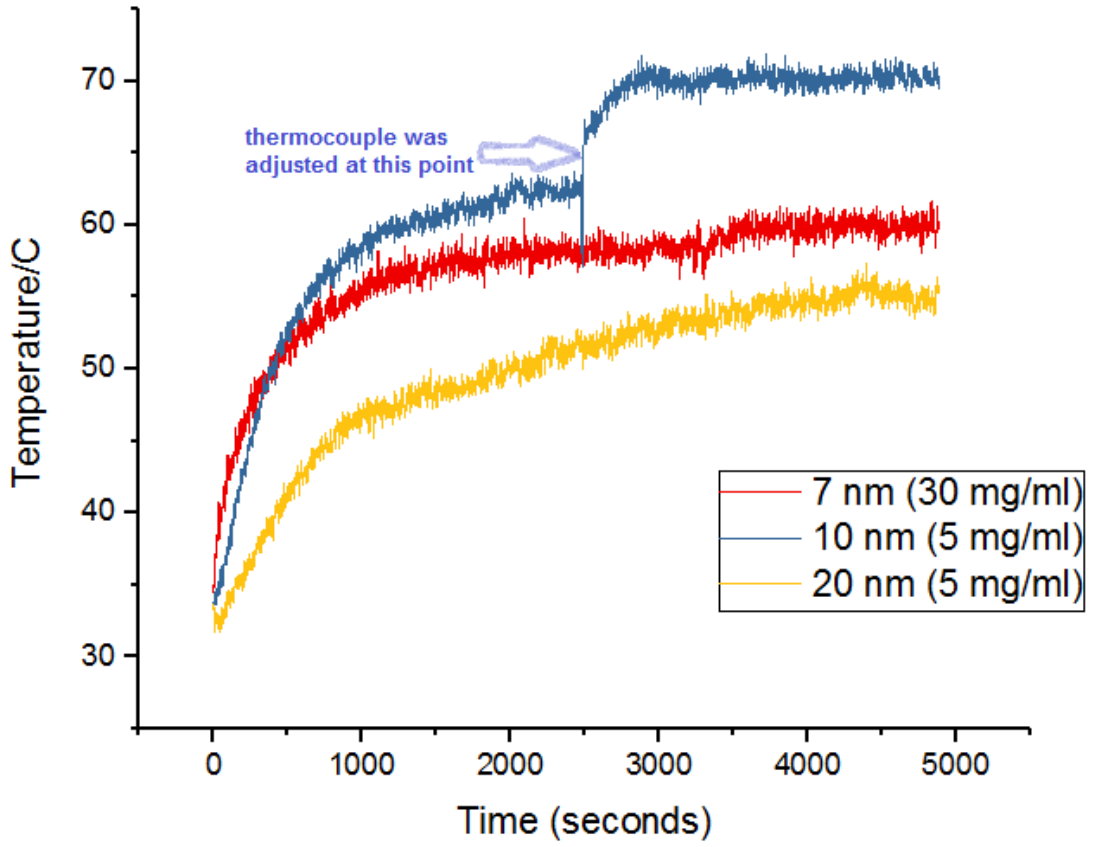

Figure 2: Time dependent temperature change curves with three different sizes of magnetic cores in olive oil.

As can be seen from the graphs, the 10 nm magnetic core had shown the maximum temperature rise. We choose this core for the synthesis of our nanoparticle.

Once the dimensions and constituents of the zinc doped iron core is decided, it is then covered with mesoporous silica to give an intermediate 'structure' before protein conjugation. For the following reasons, silica covered MCNP has several advantages over its bare counterpart as the mesoporous silica shell (a) prevents aggregation of the bare iron core particles[47]; (b) provides a homogeneous surface for the distribution of heat; (c) The reducing and oxidizing agents in the biological environments cannot react directly with iron oxide (thereby preventing Fe (II) ← → Fe(III) transition[47] .

2.2 Characterization

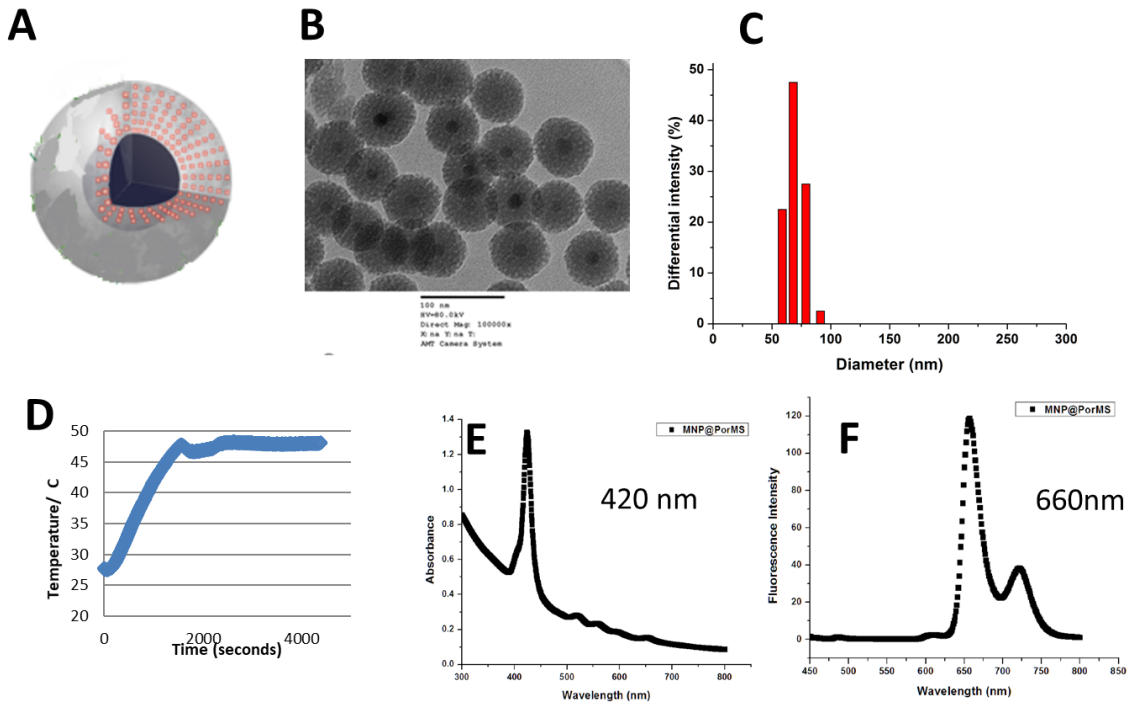

Figure 3: Characterization of Mesoporous Silica Nanoparticle with Magnetic Core
A. Artistic representation of MCNP (mesoporous silica NP with magnetic core).
B. TEM image of MCNP
C. Dynamic Light Spectroscopy (DLS) data of MCNP
D. Hyperthermia treatment of MCNP in LB broth in concentration 50 µg/ml
E. Absorption graph of MCNP (absorption maxima = 420 nm)
F. Emission graph of MCNP (emission maxima = 660 nm)

***Courtesy of Hudifah Rabie and Dr HyeonYeol Cho**

The TEM imaging showed that the overall size of the nanoparticle (bearing the $ZnFe_2O_4$ cores) range around 50 - 60 nm. Dynamic light scattering (DLS) measurements is in agreement with this data, as a significant percentage of particles are clustered around a size of 60 nm.

The resulting nanoparticle was then subjected to magnetic hyperthermia treatment (current = 42 Amperes). As can be seen, the solution temperature goes upto 48 °C when the same settings are used in the magnetic hyperthermia instrument. This indicates that the solution temperature

(physiological temperature of the cell killing) is much lower than the local surface temperature of the nanoparticles.

The nanoparticles are then subjected to fluorescence spectroscopy in the emission and absorption wavelengths expected for porphyrins. The absorption maxima occurs at 420 nm (corresponding to blue light) and the emission maxima at 660 nm (corresponding to red light). This means that the resulting nanoparticle will generate ROS when exposed to blue light; and will display red fluorescence under fluorescent microscope.

2.3 Functionalization of porphyrin:

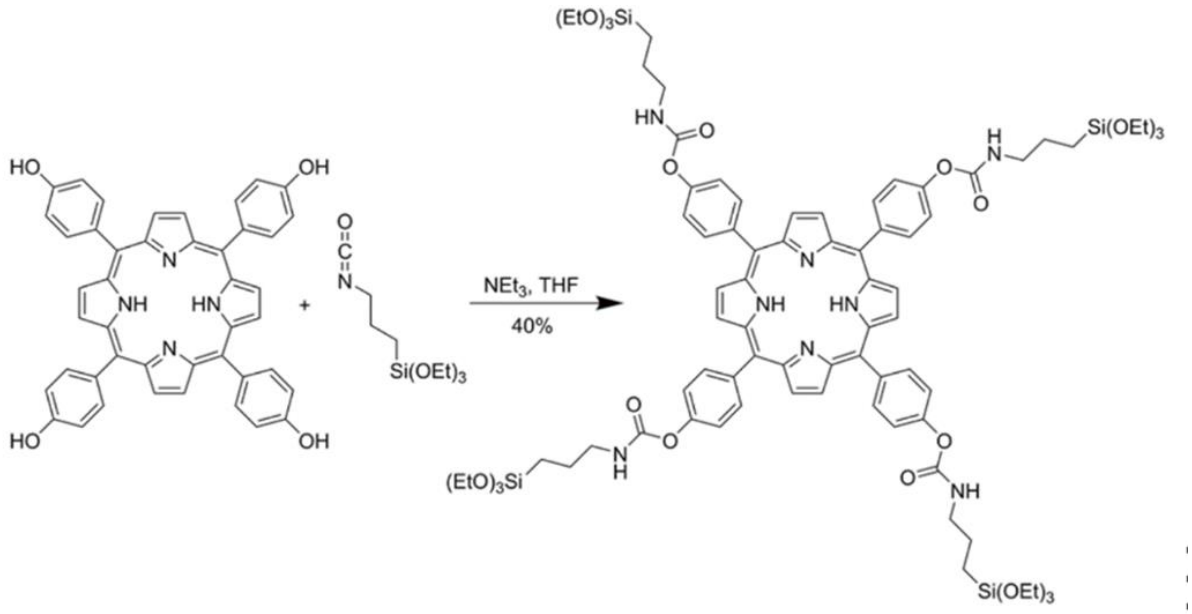

Figure 4: Synthetic route for the of porphyrin-bridged ethoxysilyl precursor.
Reprinted (adapted) with permission from Li, Y. *et al.* A photoactive porphyrin-based periodic mesoporous organosilica thin film. *Journal of the American Chemical Society* 135, 18513-18519 (2013)

Before binding with mesoporous silica, the porphyrin was functionalized using [48]. This helps the porphyrin (chemically) bind more efficiently to the mesoporous silica. Along with acting as an ROS generator, porphyrin serves as a fluorescent agent (yielding color with appropriate light exposure) thereby enabling the NanoPhage to be tracked while in treatment with bacteria.

2.4 Schematic Diagram of Nanophage Synthesis:

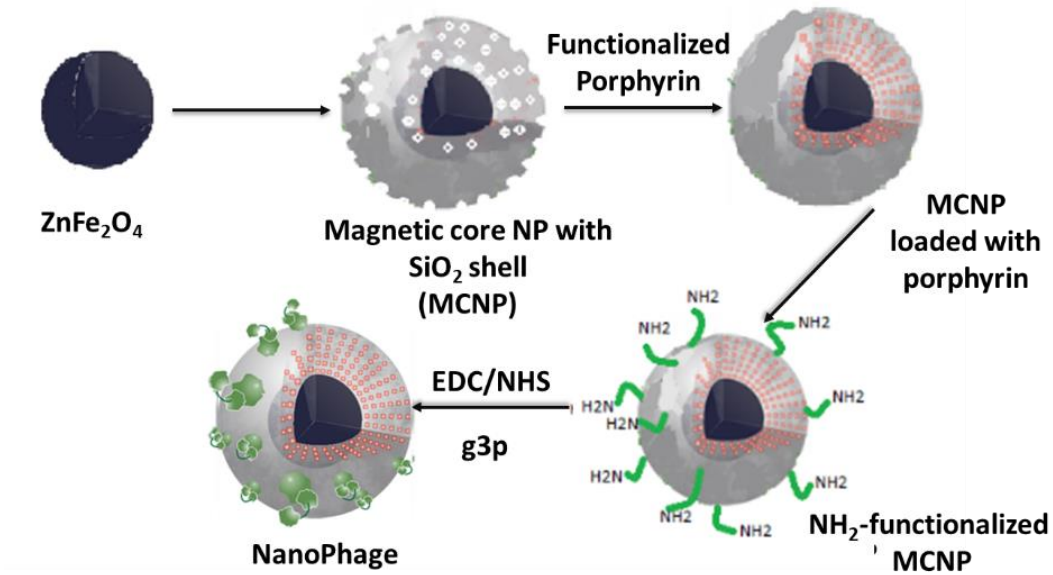

Figure 5: Schematic diagram of NanoPhage synthesis

The zinc doped iron oxide core ($ZnFe_2O_4$) coated with silica shell was synthesized, and subsequently the silica shell was functionalized by conjugating amine groups. The amine groups help in the conjugation of proteins (via peptide bonds with the carboxyl end). The amine functionalized MCNP is then treated with g3p proteins in the presence of EDC/NHS that catalyze peptide bond formation) to give a finalized 'NanoPhage' particle.

2.5 Synthesis of g3p

g3p (gene 3 protein) is a minor coat protein derived from the bacteriophage M13 that facilitates infection of *E. coli* bearing an F-pilus. Its N-terminal domain (g3p-D1) enables infection by inducing penetration of the phage into the host (E. coli) cytoplasm via interaction with the Tol complex that resides in the E. coli periplasm[34].

Filamentous Ff bacteriophages (M13, f1 and fd) infect strains of E. coli carrying an F-episome. Phage infectivity (penetration of M13 into E. coli) is known to be facilitated by the phage gene 3 protein (g3p), a minor coat protein. Three to five copies of g3p rests in one end of the extended filamentous phage particle.[34,49] The g3p protein is divided into three domains, separated by glycine-rich peptide linkers and it contains a short C-terminal transmembrane segment as shown in the figure below.

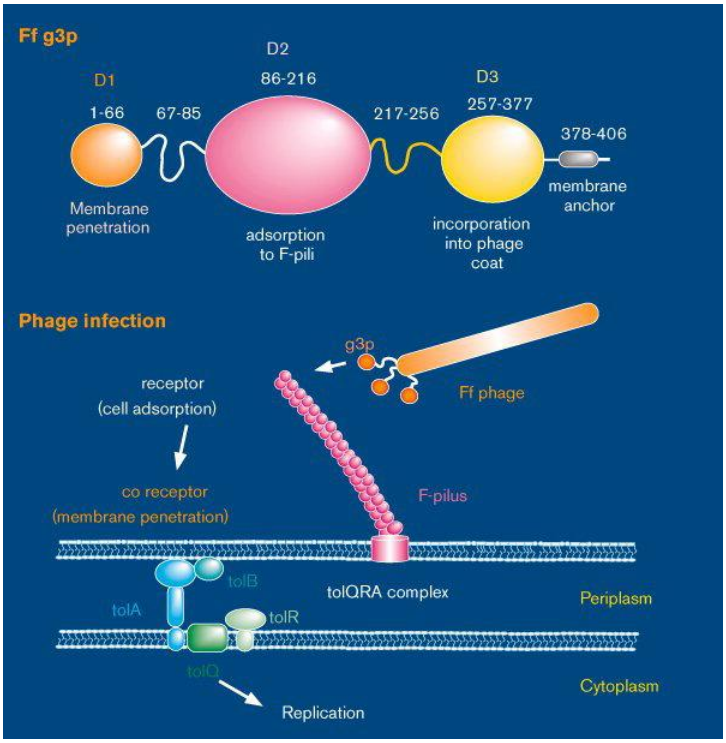

Figure 6: Schematic organization of g3p and sequence location of domains

Reprinted (adapted) with permission from Holliger, P. & Riechmann, L. A conserved infection pathway for filamentous bacteriophages is suggested by the structure of the membrane penetration domain of the minor coat protein g3p from ph age fd. *Structure* 5, 265-275, doi:Doi 10.1016/S0969-2126(97)00184-6 (1997).

The N-terminal domain (D1) is thought to be responsible for membrane penetration, the middle domain (D2) for adsorption to the F-pilus tip and the only function assigned to the C-terminal domain (D3) is the anchoring of g3p in the phage particle. The glycine rich section separating D2 and D3 are believed to have a tethering function[50]. For our project, we use the g3p

protein to coat our nanoparticle, so that it has the ability to selectively target multi drug resistant E. coli bacteria.

The expression of polyhistidine-tagged recombinant proteins in Escherichia coli, followed by affinity purification is commonly done in the laboratory[51]. The E. coli strain BL21DE3 was used for propagation of plasmids and expression of the g3p protein. Bacterial cells were grown until they reached OD_{600} value of ~0.6, and then incubated with IPTG (1mM concentration) for 24 hours; after which the cells are harvested via centrifugation and the resulting cell pellet is ultrasonicated and lysed with enzymes such as lysozyme which helps to strip the cell membrane of E. coli and yield the cells' protein contents.

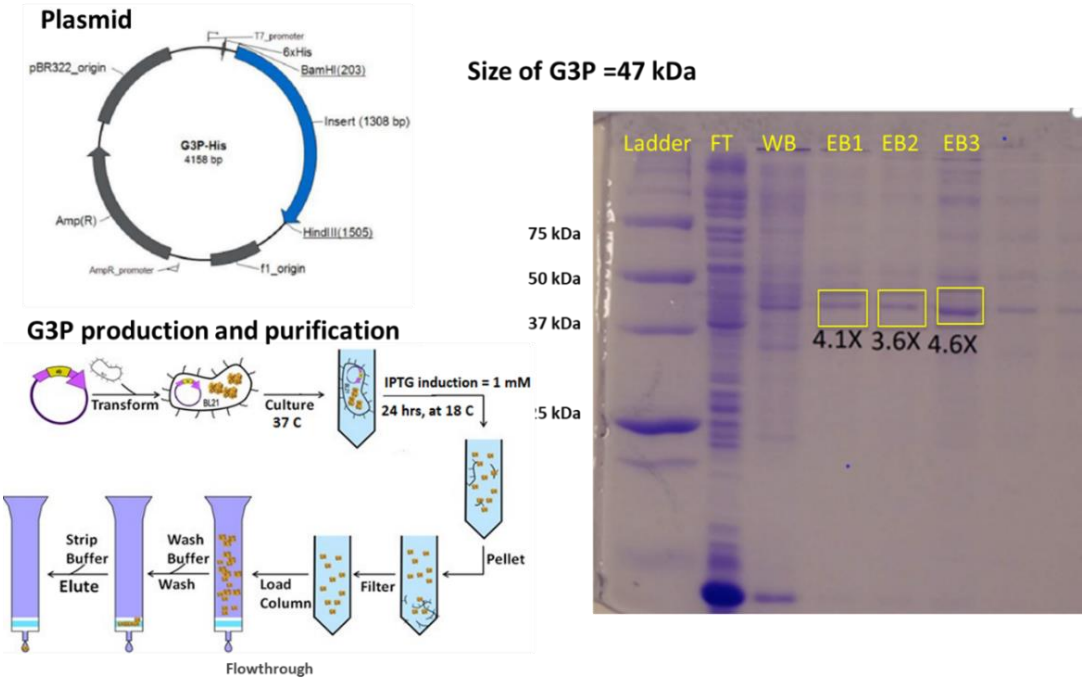

Figure 7: g3p protein synthesis and purification scheme.
A. Plasmid bearing the g3p gene
B. General purification scheme of laboratory produced proteins*
C. SDS-PAGE gel electrophoresis results showing purified g3p band (47 Da)
***Reprinted (adapted) from https://www.creative-biostructure.com/protein-purification_12.htm (accessed Oct 3, 2018)**

2.6 Purification of g3p protein:

Resins that are made of agarose beads can be functionalized with chelating groups that immobilize metal ions, which then function as ligands for the binding, followed by purification of the specific biomolecule of interest. This means for protein purification is known as immobilized metal affinity chromatography (IMAC)[52,53]. IMAC is a popular method for purifying polyhistidine affinity-tagged proteins.

The chelators that were used by our IMAC resins are nitrilotriacetic acid (NTA) and came as manufactured from ThermoFisher Scientific. The NTA-agarose resin is prepared is "loaded" with Ni^{2+} ion (Ni-NTA) resin. The binding properties of Nickel makes it suitable for specific applications of IMAC.

The low-concentration of imidazole (20 mM) in the washing buffer helps to prevent nonspecific binding of endogenous proteins that may have one or two histidine residues and have an affinity to the Nickel column.

Elution and retrieval of captured His-tagged protein from an Ni-NTA IMAC column is achieved by using a high concentration of imidazole (at least 50 mM). This ensures that proteins that have a high affinity for the Ni column (as His tagged proteins are supposed to have) is eluted.

The elution was performed in 1 ml fractions and the fractions, along with the lysate, washing buffer and flowthrough were run in an SDS Page gel electrophoresis. A band appeared in the lanes that matches the expected molecular weight of g3p (47 kDa), These data indicated that g3p protein has been produced and is purified successfully. Purified g3p (MW= 47.5 kDa) proved to be a highly soluble protein, which exhibited no tendency to aggregate at mM concentrations.

For our project, the adopted nanoparticle is conjugated with the g3p protein derived from M13 bacteriophage that normally infects E. coli. The resultant final nanoparticle is believed to have the ability to interact closely (by embedding or penetration) with E. coli cell. Hence the name 'NanoPhage' (Nanoparticle with bacterioPhage protein) has been given to the nanoparticle.

2.7 Fluorescent tagging of bacteria using g3p

Once the protein is purified, it becomes necessary to ensure that the protein interacts with the E. coli membrane in the way we hypothesized. Tagging biomolecules or nanoparticles with fluorescent probes and following their path via fluorescence microscopy is a widely used tool to investigate cellular and molecular events and get an impression about the inter- and intra-cellular dynamics of cellular processes[54]. In the next step, we therefore tag our protein with a fluorescent molecule and see how the fluorescent protein complex interacts with E. coli.

7-Amino 4-Methyl Coumarin (AMC) is a small fluorophore used for labeling free carboxyl groups of proteins. When bound to proteins, AMC radiates a fluorescence that can be detected by fluorescence microscopy[55]. This makes AMC well suited to study the interaction of proteins with bacterial cells.

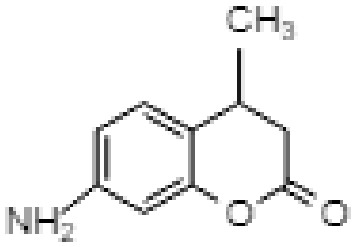

Figure 8: Molecular structure of 7-Amino 4-Methyl Coumarin (AMC)
(Drawn using ChemDraw)

The N-terminal domain of the g3p protein (g3p-D1) is thought to be responsible for E.coli membrane penetration[34], leaving the C terminal of the protein is available for binding. Therefore, a fluorophore that reacts with the C terminal was chosen to track how g3p interacts with bacteria.

EDC/NHS are widely used reagents that are used for cross linking carboxyl groups with primary amines[56] (detailed later). The same reagent and coupling reaction condition was used to cross link the C terminal domains to amine functionalized MCNP in the conjugation reaction. The AMC, together with g3p protein, in the presence of EDC/NHS are placed together in a reaction tube and rotated overnight at 4 °C allowed adequate time for AMC and g3p molecules to bind via peptide bond.

Before exposing the bacteria and proteins to fluorescence microscopy, the fluorescence spectra of g3p- AMC complex and AMC solution (at the same concentration) was taken, to ensure binding of g3p to AMC. Both solutions were excited separately at 339 nm (the characteristic excitation wavelength of AMC[57]) and both showed emissions at 439 nm (as shown below).

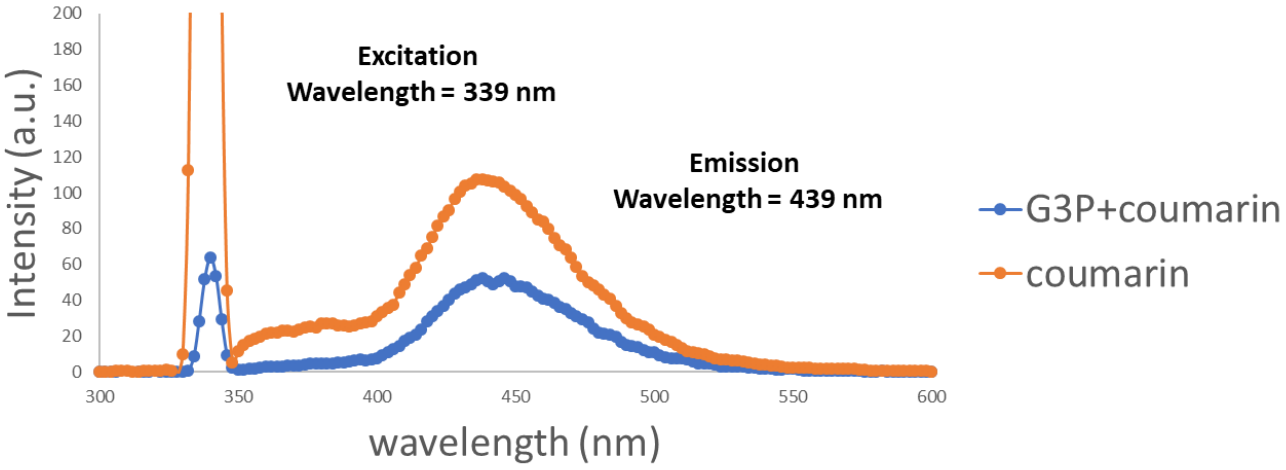

Figure 9: Emission spectra of AMC and g3p-AMC complex

That both AMC and g3p-AMC complex fluoresced at 439 nm this ensured that the g3p has successfully bound to AMC. 439 nm corresponds to blue light.

In order to create a control for the experiment, another fluorescently bound protein as used as a control (instead of G3P coumarin complex). Another protein (called LGG) was tagged

with GFP (Green fluorescent protein) and treated with E. coli in the same way. GFP is a biological marker that is used for monitoring several kinds of cellular processes. GFP can be excited by the 488 nm laser line and is optimally detected at 510 nm. Green fluorescent protein has its excitation wavelength at 395 nm, and emission wavelength a 510 nm[58], corresponding to green light. GFP does not interfere with biological processes, but can be fused to other proteins to follow their path through physiological processes. So, unlike g3p, GFP is not expected to interact with the E.coli.

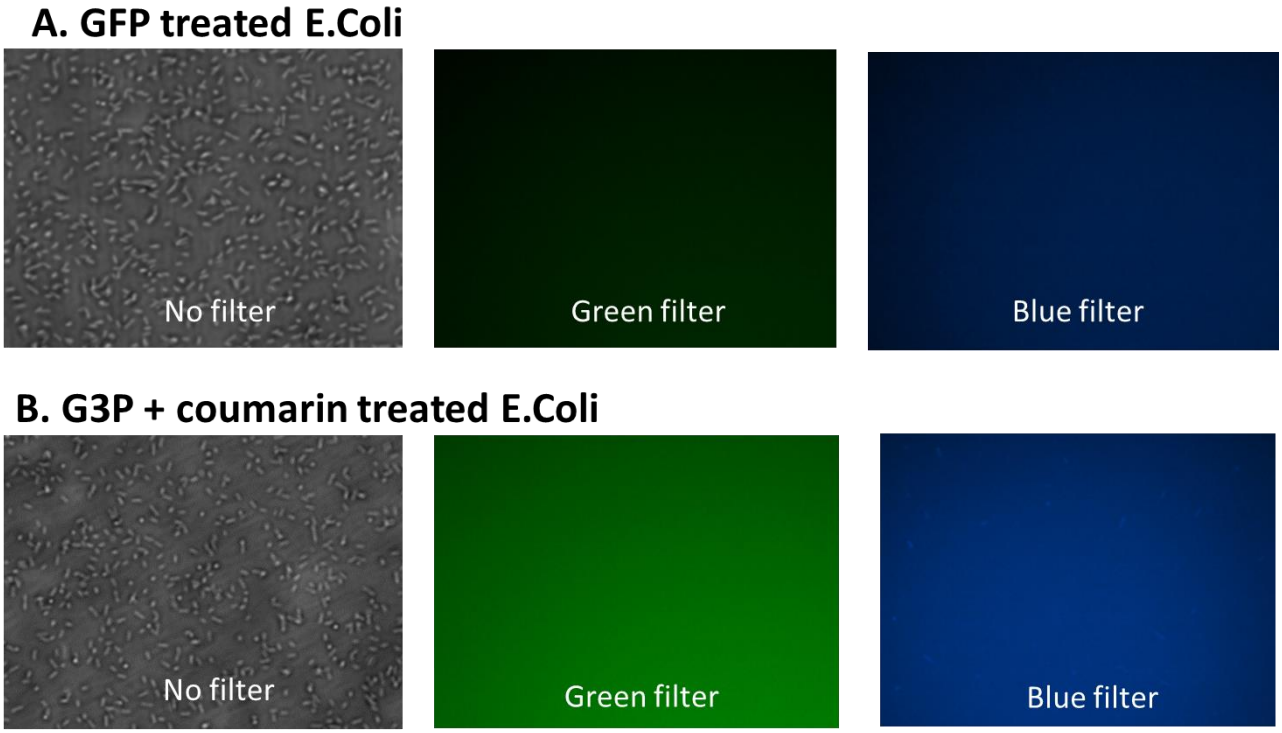

Figure 10: Fluorescent microscopic image of E. coli treated with two different proteins
A. E coli treated with GFP;
B. E. coli treated with g3p + coumarin complex

In this experiment, the E. coli was treated with protein for 2 hours and then washed with sodium phosphate buffer, and then 'fixed' using formaldehyde. The sample was then imaged under fluorescence microscope. Both samples were exposed to excitation wavelengths corresponding to GFP and AMC, and then observed to see green and blue fluorescence.

As can be seen from the results, g3p bound bacteria shows fluorescence only in blue light, E. coli treated with GFP does not fluoresce blue or green. This indicates that g3p has bound to specifically bound to E. coli membrane, whereas, GFP did not bind at all, and was washed away.

2.8 Conjugation of amine functionalized MCNP with g3p

There are two ways of preparing protein conjugated mesoporous silica nanoparticles: passive absorption[59], and covalent coupling via a linker. Although simple in preparation process, passive absorption of proteins to nanoparticles is not efficient as protein molecules may desorb from the surface over time. In addition, in many cases, the proteins fail to retain their intrinsic properties after being absorbed to the surface, which can be caused by changes in tertiary structure or nonspecific binding of proteins to the nanoparticle surface.

One possible way to circumvent the problem would be to covalently couple protein molecules to amine functionalized nanoparticles. This method provides much enhanced stability of the protein coating compared to the passive absorption method. Covalent coupling makes use of 'linkers' that react with specific chemical groups on protein molecules and the functionalized nanoparticles. Therefore, the method is provides greater specificity.

We rely of EDC/NHS chemistry for the conjugation of g3p protein molecules to amine functionalized mesoporous silica nanoparticles. EDC/ NHS complex reacts with amine groups on the particle surface to form an intermediate that can subsequently react with carboxylate groups of g3p. The efficiency of EDC/NHS conjugation reaction is known to be low, so we add a 10X excess of EDC/NHS.This method, also known as one -step conjugation, provides a relatively simple method of conjugating proteins to nanoparticles. Because of its short half-life, it is necessary to freshly prepare EDC/NHS just before conjugation. Effective removal of excess EDC/NHS after conjugation is done by washing using sodium phosphate buffer.

Once conjugated with proteins, our nanoparticle has completed its final stage of synthesis before being treated with bacteria.

2.9 Heat treatment of bacteria

Heat treatment is one of the most widely used methods for causing the death of pathogenic bacteria. Mild-heat treatment, known as pasteurization, is widely used for getting rid of bacteria from food items. An understanding of the mechanism and kinetics of thermal death of bacteria has been studied in the past[60] by various methods[61].

During this process of heating, the cell proceeds from a living state to a death state. Heat can be applied as moist or dry heat. Dry heat (i.e. where water is not a medium of heat transfer) is known to kill microbes by oxidizing the molecules[61]. Moist heat transfers heat energy to the microbial cells more efficiently and kills microbial cells by denaturing enzymes.[61] The moist heat method includes boiling, pasteurization and autoclaving.

Heat damages cellular proteins by breaking the covalent and H-bonds that link the adjoining portions of amino acid chains and maintain the three-dimensional shapes of globular proteins, (like enzymes) that is necessary for its function[61].

Heat treatment also said to cause inactivation of 'critical sites' in the cellular membranes of bacteria. The damage to the cell membrane results in the leakage of potassium, amino acids, and nucleotides or nucleic acids, and the loss of salt tolerance, and allows diffusion of toxic agents which cannot pass through an undamaged cell membrane[60].

For our project, to note the temperature which causes the death of E. coli bacteria due to heating, we design an experiment where we can both measure and control the temperature E. coli is subjected to, as opposed to hyperthermia, in which the 'registered temperature' is very different from the local temperature of nanoparticle attached to cells. This experiment gives us a good

estimate of the temperature at which E. coli must be subjected to achieve optimal killing efficiency. We do this experiment by subjecting E. coli bacteria to water bath treatment at specific temperatures of 5 °C increments.

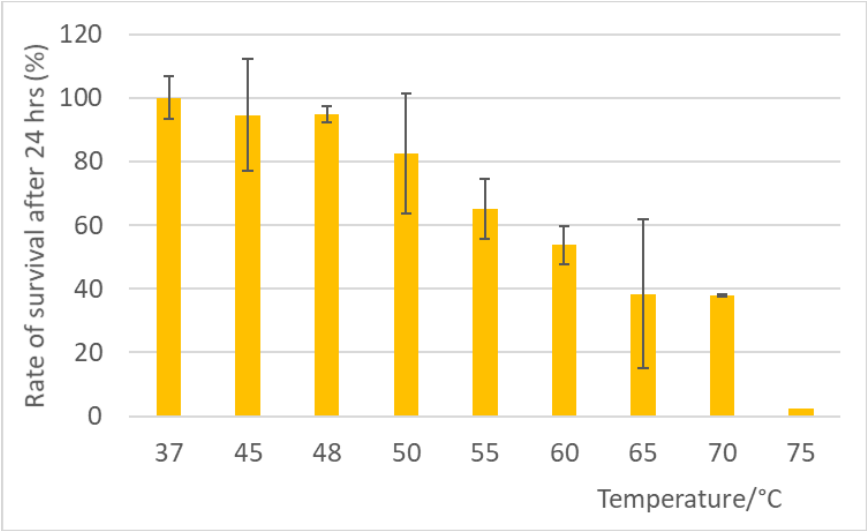

Figure 11: Temperature dependent killing of E. coli BL21DE3

As can be seen from the graph, the survival rate of bacteria decreases with increasing temperature; the temperature that results in absolute cell killing is 75 °C. This suggests that for the hyperthermia to result in cell death, the surface temperature of the NanoPhage needs to be much higher than the temperature commonly used for hyperthermia to achieve significant killing efficiency.

2.10 Killing E. coli using NanoPhage

NanoPhage is expected to interact with the bacterial cell membrane using g3p protein conjugated on its surface (either by sticking on the cell surface or by penetration). Subjecting the nanoparticle to magnetic hyperthermia heats up the nanoparticle surface and raises the temperature of bacterial cells by convection; ROS generated by porphyrin causes free radical

generation. Therefore, a combination of magnetic hyperthermia and ROS generation enables NanoPhage in proximity of E. coli proteins to kill bacteria very efficiently.

Magnetic hyperthermia is a well-researched method for the past few decades as a method to selectively kill cells using magnetic field. Magnetic nanoparticles subjected to hyperthermia convert magnetic energy (generated by a coil) to heat energy under an AC magnetic field via a mechanism called magnetic hysteresis[62]. Magnetic hyperthermia has been researched extensively for cancer therapy for its selective ability to kill cells.

The heat generated by hyperthermia mainly has its effects on various kinds of proteins in the cell body and the cell surface membrane of cells targeted by magnetic core nanoparticles (MCNP). As soon as the MCNP reaches a specific temperature, the cells heat up by convection and proteins start to unfold, exposing their hydrophobic groups – ultimately resulting in aggregation[37]. This causes the proteins to aggregate, impeding cellular function. Having similar effects on the proteins on the plasma membrane affects the permeability of plasma membranes resulting in ionic imbalance. In the mitochondrial membrane, there is a change in the redox status of cells

Although hyperthermia does not directly cause DNA damage, hyperthermia treatment changes the associations of nuclear proteins, particularly those involved in DNA replication – thus making it much less likely for cells to reproduce or transcribe proteins necessary for survival and cell division.

The types of cell death induced by hyperthermia are classified as heat induced apoptosis[63], mitotic catastrophe secondary to alterations in the proteins that support DNA metabolism[64,65]. The type of cell death is highly cell-type and temperature dependent[66], most cell lines die of a combination of death processes.

We subject E. coli to hyperthermia treatment after incubation with NanoPhage. Amine functionalized MCNP that was used as a control - since similar nanoparticles have been used as killing agents in previously reported literature, it is easier to get comparative killing data compared to previously reported values.

The typical temperature for magnetic hyperthermia that is used to kill cancer cells is between 41 °C to 43 °C. This temperature range is within what is known as moderate hyperthermia. For this reason, initially, we chose a temperature of 42 °C to test on our bacterial cells. Although significantly fewer macromolecular changes occur in the 40.5 C to 42C range, these changes are still numerous and occur in multiple cellular compartments.

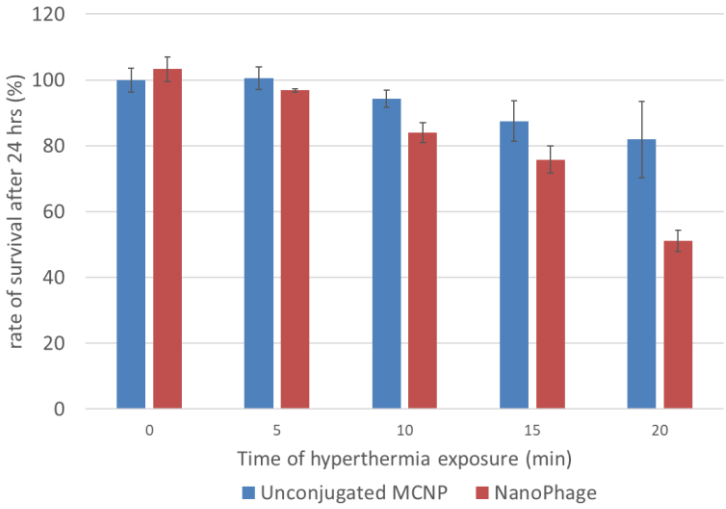

Figure 12: Survival rate of E. coli BL21DE3 at 42 ° C 24 hours after hyperthermia treatment

As can be seen, after 20 minutes of treatment, the rate of survival of NanoPhage after 24 hours is slightly higher than 50%. Ideally, this is a very high survival rate for any antibacterial therapy. In literature, cell survival curves for temperatures of 42.5 °C shows an exponential cell

death followed by a plateau. The cause of this phenomena is attributed to the development of chronic thermal tolerance[67].

In contrast, it has been long recognized that hyperthermia in the 43–47C temperature range kills cells more efficiently, without a shoulder. We therefore choose to use a higher temperature for i.e. 48 °C, for our next set of cell killing data collection.

Another key point to note is how the amine functionalized MCNP (without the g3p protein conjugated on its surface) also shows notable bacteria killing. This is because in an aqueous environment, the amine groups on the surface become protonated and positively charged (NH_3^+), rendering the MCNPs an overall positive charge. Since the cell membrane of bacteria is negatively charged, the MCNPs bind to the bacterial cell surface by electrostatic attraction. That is why, some killing does occur by unconjugated MCNP.

At a temperature range of 40–47 °C cause proteins to be unfolded, exposing hydrophobic groups, which can then interact forming aggregates[67]. In principle, these heat effects on proteins are reversible by the presence of molecular chaperones[68,69]. At a higher temperature 48 °C ad above, proteins undergo thermal ablation, that results in severe irreversible protein denaturation[70].

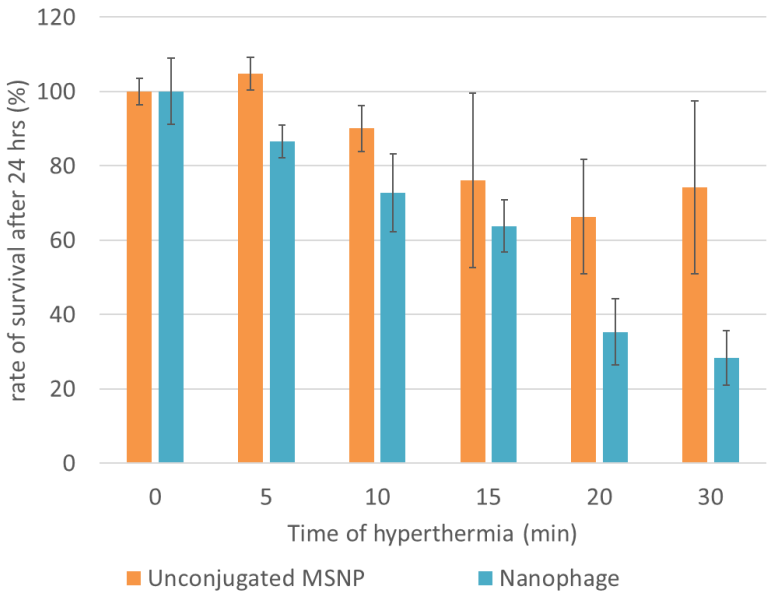

Figure 13: Survival rate of E. coli BL21DE3 at 48 °C 24 hours after hyperthermia treatment

Although hyperthermia is not believed to cause direct DNA damage, it is assumed that but increase in temperature is believed to cause heat effects on proteins involved in DNA replication, chromosome segregation and DNA repair .

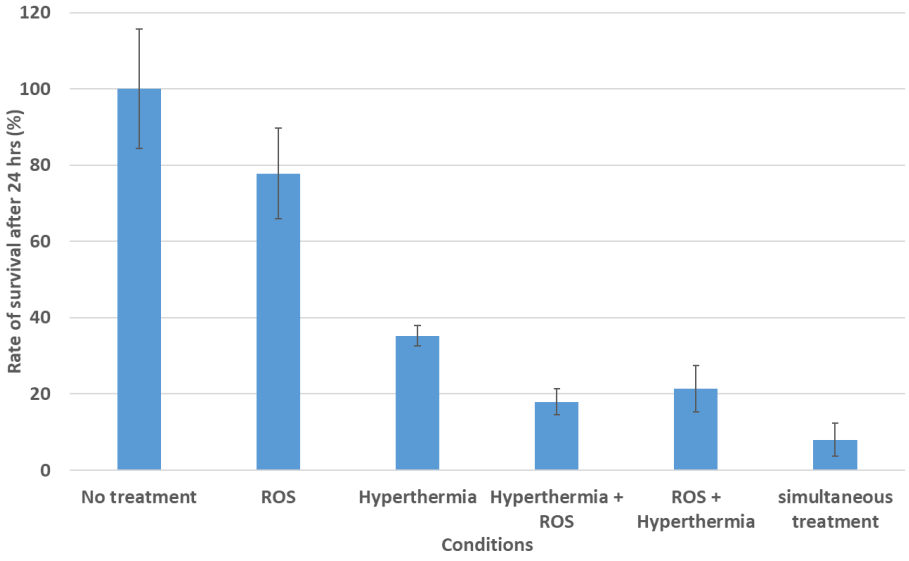

Figure 14: Survival rate of E. coli BL21DE3 at 48 °C 24 hours after hyperthermia treatment with different conditions.

In order to improve efficiency of killing, we then subject the E. coli to hyperthermia killing with photodynamic therapy. As noted before, the mesoporous silica shell of NanoPhage is also packed with porphyrin molecules that are able to generate Reactive Oxygen Species (ROS) when exposed to blue light (420 nm). Interaction between the triplet excited state of the porphyrin and molecular oxygen leads to produce singlet oxygen and other ROS to induce cell death[40]. Five different experimental conditions were used when bacteria were treated with hyperthermia in combination with ROS therapy while hyperthermia only (48 °C), MCNPs only, NanoPhage with hyperthermia, or RF with heat resulted in inadequate killing activity.

The ROS + hyperthermia therapy, in which magnetic hyperthermia was performed on the bacteria at the same time of exposing to blue light (420 nm) for 30 minutes, gave the best killing efficiency (7% survival rate of bacteria in 24 hours). T is very likely that the degradation of protein on the cell surface membrane of bacteria weakens the cell membrane, thereby making it easier for proteins in the cell to be killed by ROS generated by porphyrin. This proves that hyperthermia and photodynamic therapy complement each other in cell killing.

Chapter 3:

Materials and Methods

3.1 Synthesis of Zn-Doped Iron Oxide Nanoparticles

In a typical experiment for synthesis of MCNP, zinc chloride ($ZnCl_2$) was taken together with iron(III) acetylacetonate ($Fe(acac)_3$, $C_{15}H_{21}FeO_6$), oleic acid, oleylamine, and 1,2-hexadecanediol were mixed of trioctylamine in a 100 mL three-neck round-bottom flask. The reaction mixture was heated to 200 °C for 2 hours, after which the temperature was increased to 300 °C. After 1 hour, the reaction mixture was cooled to room temperature and the MCNPs were precipitated using ethanol. They were purified by repeated centrifugation and sonication. The as-obtained nanoparticles were then dried overnight under vacuum[71].

3.2 Functionalization of porphyrin using ethoxysilyl

A derivative of porphyrin - meso-tetra(p-hydroxy)phenyl porphyrin was obtained commercially and taken with dry THF in a Schlenck tube. 3-isocyanatopropyltriethoxysilane and TEA were added to the solution at room temperature in the absence of oxygen. The reaction mixture was heated to 80 °C for 4 h. After concentration in vacuo, filtration and washing with ethylacetate all volatiles products were disposed. The resulting oily residue was taken up in little ethy acetate and made to precipitate with hexanes. The mixture was centrifuged five times and the precipitate collected The resulting solid was dried under high vacuum to obtain the coumpound[48].

3.3 Heating efficiency of $ZnFe_2O_4$ iron cores

In order to obtain an estimate of the surface temperature of MCNPs, the 5 nm, 10 nm, and 15 nm zinc doped iron oxide ($ZnFe_2O_4$) nanoparticles sediment was obtained, and were suspended

olive oil to form mixtures of 30 mg/mL and 5 mg/mL. The mixtures were sonicated to create evenly dispersed oil-NP mixtures. Hyperthermia was carried out in the same conditions that is used for bacteria killing (53 A, 5 turn coil), and the temperature rise recorded over a period of nearly 2 hours to record maximum temperature reached.

3.4 Synthesizing the G3P protein

3.4.1 Making the preculture

A cell culture stock (stored in glycerol in a 1 ml microtube) was obtained from -80℃ freezer. A small amount of bacteria was streaked using a pipette tip, and placed in a 15 mL tube with 5 mL of autoclaved LB broth and 5.0 ul 1000X ampicillin (final concentration 100 ug/ml). The pre-culture was left overnight in incubating shaker at 37°C, 250 rpm.

3.4.2 Expanding the preculture

In a 600 mL culture flask, 150 mL of LB broth, 1.5 mL of grown preculture, and 5 uL 1000X ampicillin (final concentration 100 ug/ml) were taken. The expansion was allowed to grow in the shaking incubator at 37°C, 250 rpm, and the OD (Optical Density) value was monitored within this time with a UV-Vis spectrometer. When the OD value reached 0.5-0.6 (in 3 to 4 hours), IPTG was then added to the culture (final concentration 1 mM) and the expansion was kept shaking in the incubator at 18 °C for 24 hours.

After 24 hours, the expansion was centrifuged down at 4°C, 7500 rpm, 5 min and washed with phosphate buffer 3 times.

3.4.3 Lysing cells

The cell stock was placed in ice, and 13 mL of 1X PBS buffer was added, along with 1.5 mL of PMSF (final concentration 1 mM). The cells were vortexed to be resuspended, and lysed using an ultrasonicator (7 watts, 10 x 30 sec. rounds with 30 sec. breaks (5 minutes total, amplitude 40%). Lysozyme was added to cells (final [lysozyme] = 2 mg/mL) to facilitate lysis and the sample was incubated in ice for one hour. The sample was sonicated again (7 watts, 10 x 30 sec. rounds with 30 sec. breaks (9 minutes total), amplitude 50%).

The lysate was centrifuged at (4°C, 13300 rpm for 30 mins. The supernatant was collected and syringed with a 0.22 um filter.

3.4.4 IMAC column chromatography

Recipes for:

Wash buffer 1 = 1X PBS, pH 7.4

Wash buffer 2 = 1X PBS, pH 7.4, 20mM Imidazole

Elution buffer = 1X PBS, pH 7.4, 200mM Imidazole

1 X PBS = 137mM NaCl, 2.7mM KCl, 10mM Na_2HPO_4, 2mM KH_2PO_4

2-3 mL of resin loaded with Ni ions was purchased from ThermoFisher and loaded onto a column. The resin was the then washed with 30 mL of DI water, and then Washing buffer 1 was allowed to run through the resin (to equilibrate the ion concentration) by gravity flow at a rate of about 1 ml/min of a column with a bed diameter of ~ 7 mm (1 ml HisTrap or Ni-NTA Superflow Cartridges).

The protein was then loaded onto the resin and incubated overnight by end -over -end rotation to maximize his-tagged protein binding. The lysate was allowed to run in the column in the same way (gravity flow) and the FlowThrough was collected.

The Ni-NTA column was then washed with a low concentration (20mM) of imidazole containing washing buffer (Washing Buffer 2).

The His-tagged protein was then eluted with Elution buffer (imidazole concentration 50 mM to 200 mM) and collected in 1 mL fractions.

The resin can be washed with EDTA (to elute all Nickel ions) and reloaded with NiSO4 solution to be reused for another cycle of His-tagged protein purification at a later date.

3.5 Conjugation of proteins with Nanoparticles*:*

In 500ul MCNP@mSI-NH2, 0.458mg NHS, 0.62mg EDC in 300 uL of PBS buffer was added. 200ul G3P solution (0.6mg/ml) was added dropwise, and the mixture stirred with a magnetic stirrer for 12 hours at 4°C, in the absence of light (by covering with Al foil). After the 12-hour incubation, the mixture was centrifuged at 6000 rpm for 10 minutes and the supernatant was disposed. The pellet was washed three times with PBS buffer, re-dispersed in 1 mL PBS buffer and stored at 4°C, in the absence of light.

3.6 Fluorescence tagging of bacteria using g3p:

800 uL of G3P (0.45 mg/mL) was incubated with 20 uL of 10 mg/mL solution of 7-Amino 4 methyl coumarin (AMC) dissolved in DMSO. 1.2 mL of EDC (2.48 mg)/NHS (1.92 mg) solution was added (as crosslinking agent). The mixture was incubated overnight in a rototar to maximize binding of the C terminal of G3P protein with the amine group of coumarin. After overnight incubation, the G3P- tagged protein was extensively dialyzed though a 10,000 M.W.C.O filter

(Millipore) and a buffer exchange was performed with sodium phosphate buffer. The final concentration of protein in the solution was 0.18 mg/mL as measured by Bradford assay.

A preculture of kanamycin resistant E. coli without the g3p plasmid was grown (as explained above). The preculture was diluted 10 X to an OD value of ~ 0.2. 500 uL of the diluted preculture was taken in a 1.7 mL minitube and incubated with 500 uL of protein solution, as in the following setting:

a) 500 uL of diluted preculture + 500 uL of 0.2 mg/mL G3P tagged with coumarin
b) 500 uL of diluted preculture + 250 uL of 0.4 mg/mL of GFP tagged protein + 250 uL of PBS.
c) 500 uL of diluted preculture + 500 uL of PBS buffer.

Final concentration of proteins in the a) and b) were 0.1 mg/mL.

The three tubes were incubated for 2 hours in a rotor. They bacteria in the tubes were then centrifuged down (13,300 rpm, 10 mins), and the cell pellet 'fixed' by incubating with formaldehyde for one hour. The bacteria were then spinned down with the same settings and washed with phosphate buffer three times.

3.7 Heat treatment of bacteria using water bath:

A preculture of E. coli was grown (as described in),and diluted to an OD value of 0.04. 1 mL of this diluted preculture was pipetted into 21 tubes each (three tubes for each temperature treatment). The tubes were then subjected to treatment of 37°C, 45°C, 50°C, 55°C, 60°C, 70°C and 75°C for 15 minutes, and then incubated t 37°C for 24 hours. The OD value of the cultures were then recorded.

3.8 Killing E. coli using NanoPhage by Magnetic Hyperthermia and/or Photodynamic therapy:

A preculture of E. coli bacteria was prepared (as described above). The preculture was diluted to an OD_{600} value of 0.04 (measured using a UV-Vis instrument).

3.8.1 Nanoparticle uptake by incubation

The MCNP conjugated with g3p protein (NanoPhage) was retrieved from the refrigerator (stored at 4 °C), and sonicated. The control that was decided on was unconjugated MCNP (that w and suspended with diluted preculture. For a desired particle concentration (50 µg/ml or 100 µg/ml).

3.8.2 Incubation

The resulting NanoPhage +diluted E. coli solution was incubated at 4 °C by rotating in a rotor. The solution was equally distributed in 5 separate tubes and the tubes labeled with respect to the time each tube is expected to be in the hyperthermia: 0 mins, 5 mins, 10 mins, 15 mins, 20 mins.

3.8.3 Hyperthermia

After exactly 2 hours of incubation of E. coli + NanoPhage, the tubes were placed in the hyperthermia coil and exposed to hyperthermia until each sample reached a specific temperature. The temperature was maintained for the specifies length of time.

The tubes were taken out of the hyperthermia instrument, and the OD600 values recorded. The tubes were then placed in a rack and transferred to a shaking incubator at 37 C for 24 hours. The OD600 values were also recorded after 24 hours

Chapter 4:

Conclusion:

This project involved using a known structure of a commonly used nanoparticle improvised with proteins derived from bacteriophage to kill multi drug resistant bacteria. The protein that is used by the bacteriophage M13 to penetrate into the cell body of the E. coli was identified and isolated to be conjugated on the surface of the nanoparticle for efficient interaction (possible penetration) of the nanoparticle into the bacteria cell membrane.

To maximize killing efficiency, we had to choose for a specific diameter of an iron-based core, purify proteins to beconjugated on the nanoparticle, prove the protein's binding efficiency, and check the killing efficiency of the particle using magnetic hyperthermia at two different temperatures and simultaneous treatment with ROS

The bacterial solution treated with nanoparticles were exposed to hyperthermia (and /or photodynamic therapy for ROS generation) and the rate of growth measured my UV-Vis spectroscopy. The control used was the non -protein conjugated amine functionalized MCNP. The OD_{600} values were normalized against 'no treatment' conditions to demonstrate how the growth of bacteria compares to control conditions. Two temperature conditions were chosen: 42 °C and 48 °C. A higher surface temperature of the nanoparticles at 48 °C hyperthermia exposure killed the bacteria much more efficiently than at 42 °C.

Our approach is novel in that for the first time to our knowledge, proteins extracted from bacteriophage were used to conjugate onto nanoparticles to selectively target bacteria. In doing so,

we were able to mimic the naturally occurring bacterial killing strategy of bacteriophage using nanoparticles.

In previously reported literature, the amine functionalized nanoparticle with similar structure was used to show significant bacterial killing efficiency. Our approach uses a much lower concentration of the xenobiotic to achieve a similar effect. It is possible to get rid of bacteria by using magnetic hyperthermia and porphyrin. Hyperthermia and photodynamic therapy, when used synergistically, complement each other in cell killing.

Two major problems that still remain are that we have (not yet) been able to show 100% killing efficiency (corresponding to 0% survival rate) and that our nanoparticle has not been tested on other strains of bacteria to confidently state that our nanoparticle is only selective towards killing E. coli bacteria. The former problem can possibly be solved by using a higher concentration of NanoPhage for our experimentation. Though at present we are unable to give an estimation of what the concentration of the nanoparticles that results in more efficient killing, our results provide a basis for using nanoparticles conjugated with proteins from bacteriophage for effective bacterial killing. However, it is imperative that the flexibility of nanoparticle interaction and their influence on other bacterial strains be explored.

References

1 Spellberg, B. *et al.* The epidemic of antibiotic-resistant infections: a call to action for the medical community from the Infectious Diseases Society of America. *Clin Infect Dis* **46**, 155-164, doi:10.1086/524891 (2008).

2 Neu, H. C. The crisis in antibiotic resistance. *Science* **257**, 1064-1073 (1992).

3 Toprak, E. *et al.* Evolutionary paths to antibiotic resistance under dynamically sustained drug selection. *Nature Genetics* **44**, 101-U140, doi:10.1038/ng.1034 (2012).

4 Witte, W. Medical consequences of antibiotic use in agriculture. *Science* **279**, 996-997, doi:DOI 10.1126/science.279.5353.996 (1998).

5 Andersson, D. I. & Hughes, D. Antibiotic resistance and its cost: is it possible to reverse resistance? *Nature Reviews Microbiology* **8**, 260-271 (2010).

6 Ventola, C. L. The antibiotic resistance crisis: part 1: causes and threats. *Pharmacy and Therapeutics* **40**, 277 (2015).

7 Davies, J. & Davies, D. Origins and evolution of antibiotic resistance. *Microbiol Mol Biol Rev* **74**, 417-433, doi:10.1128/MMBR.00016-10 (2010).

8 Ochman, H., Lawrence, J. G. & Groisman, E. A. Lateral gene transfer and the nature of bacterial innovation. *Nature* **405**, 299-304, doi:10.1038/35012500 (2000).

9 Nachega, J. B. & Chaisson, R. E. Tuberculosis drug resistance: a global threat. *Clin Infect Dis* **36**, S24-30, doi:10.1086/344657 (2003).

10 Friedland, I. R. & McCracken, G. H., Jr. Management of infections caused by antibiotic-resistant Streptococcus pneumoniae. *N Engl J Med* **331**, 377-382, doi:10.1056/NEJM199408113310607 (1994).

11 Lee, J. H., Jeong, S. H., Cha, S.-S. & Lee, S. H. A lack of drugs for antibiotic-resistant Gram-negative bacteria. *Nature Reviews Drug Discovery* **6** (2007).

12 Allen, H. K., Trachsel, J., Looft, T. & Casey, T. A. Finding alternatives to antibiotics. *Annals of the New York Academy of Sciences* **1323**, 91-100 (2014).

13 Huh, A. J. & Kwon, Y. J. "Nanoantibiotics": a new paradigm for treating infectious diseases using nanomaterials in the antibiotics resistant era. *Journal of Controlled Release* **156**, 128-145 (2011).

14 Whitesides, G. M. Nanoscience, nanotechnology, and chemistry. *Small* **1**, 172-179 (2005).

15 Hajipour, M. J. *et al.* Antibacterial properties of nanoparticles. *Trends in biotechnology* **30**, 499-511 (2012).

16 Mahmoudi, M. & Serpooshan, V. Silver-coated engineered magnetic nanoparticles are promising for the success in the fight against antibacterial resistance threat. *ACS nano* **6**, 2656-2664 (2012).

17 Park, H. *et al.* Inactivation of Pseudomonas aeruginosa PA01 biofilms by hyperthermia using superparamagnetic nanoparticles. *Journal of microbiological methods* **84**, 41-45 (2011).

18 Pan, X. *et al.* Mutagenicity evaluation of metal oxide nanoparticles by the bacterial reverse mutation assay. *Chemosphere* **79**, 113-116 (2010).

19 Wang, S., Lawson, R., Ray, P. C. & Yu, H. Toxic effects of gold nanoparticles on Salmonella typhimurium bacteria. *Toxicology and industrial health* **27**, 547-554 (2011).

20 Juan, L., Zhimin, Z., Anchun, M., Lei, L. & Jingchao, Z. Deposition of silver nanoparticles on titanium surface for antibacterial effect. *International journal of nanomedicine* **5**, 261 (2010).

21 Friedman, A. *et al.* Susceptibility of Gram-positive and-negative bacteria to novel nitric oxide-releasing nanoparticle technology. *Virulence* **2**, 217-221 (2011).

22 Gajjar, P. *et al.* Antimicrobial activities of commercial nanoparticles against an environmental soil microbe, Pseudomonas putida KT2440. *Journal of Biological Engineering* **3**, 9 (2009).

23 Panyala, N. R., Pena-Mendez, E. M. & Havel, J. Silver or silver nanoparticles: a hazardous threat to the environment and human health? *J Appl Biomed* **6**, 117-129 (2008).

24 Stewart, P. S. Mechanisms of antibiotic resistance in bacterial biofilms. *International Journal of Medical Microbiology* **292**, 107-113 (2002).

25 Haq, I. U., Chaudhry, W. N., Akhtar, M. N., Andleeb, S. & Qadri, I. Bacteriophages and their implications on future biotechnology: a review. *Virology journal* **9**, 9 (2012).

26 Putnam, F. W. Bacteriophages: nature and reproduction. *Advances in protein chemistry* **8**, 175-284 (1953).

27 Alisky, J., Iczkowski, K., Rapoport, A. & Troitsky, N. Bacteriophages show promise as antimicrobial agents. *Journal of Infection* **36**, 5-15 (1998).

28 Sulakvelidze, A., Alavidze, Z. & Morris, J. G. Bacteriophage therapy. *Antimicrobial agents and chemotherapy* **45**, 649-659 (2001).

29 Carlton, R. M. Phage therapy: past history and future prospects. *ARCHIVUM IMMUNOLOGIAE ET THERAPIAE EXPERIMENTALIS-ENGLISH EDITION-* **47**, 267-274 (1999).

30 Lu, T. K. & Koeris, M. S. The next generation of bacteriophage therapy. *Current opinion in microbiology* **14**, 524-531 (2011).

31 Chernomordik, A. Bacteriophages and their therapeutic-prophylactic use. *Meditsinskaia sestra* **48**, 44-47 (1989).

32 Drulis-Kawa, Z., Majkowska-Skrobek, G., Maciejewska, B., Delattre, A.-S. & Lavigne, R. Learning from bacteriophages-advantages and limitations of phage and phage-encoded protein applications. *Current Protein and Peptide Science* **13**, 699-722 (2012).

33 Gelperina, S., Kisich, K., Iseman, M. D. & Heifets, L. The potential advantages of nanoparticle drug delivery systems in chemotherapy of tuberculosis. *American journal of respiratory and critical care medicine* **172**, 1487-1490 (2005).

34 Holliger, P. & Riechmann, L. A conserved infection pathway for filamentous bacteriophages is suggested by the structure of the membrane penetration domain of the minor coat protein g3p from phage fd. *Structure* **5**, 265-275, doi:Doi 10.1016/S0969-2126(97)00184-6 (1997).

35 Lubkowski, J., Hennecke, F., Pluckthun, A. & Wlodawer, A. The structural basis of phage display elucidated by the crystal structure of the N-terminal domains of g3p. *Nat Struct Biol* **5**, 140-147 (1998).

36 Shah, R. R. *et al.* Determining iron oxide nanoparticle heating efficiency and elucidating local nanoparticle temperature for application in agarose gel-based tumor model. *Materials Science and Engineering: C* **68**, 18-29 (2016).

37 van Loo, G. *et al.* The role of mitochondrial factors in apoptosis: a Russian roulette with more than one bullet. *Cell death and differentiation* **9**, 1031 (2002).

38 Kumar, C. S. & Mohammad, F. Magnetic nanomaterials for hyperthermia-based therapy and controlled drug delivery. *Advanced drug delivery reviews* **63**, 789-808 (2011).

39 Raaphorst, G., Freeman, M. & Dewey, W. Radiosensitivity and recovery from radiation damage in cultured CHO cells exposed to hyperthermia at 42.5 or 45.5 C. *Radiation research* **79**, 390-402 (1979).

40 Kou, J., Dou, D. & Yang, L. Porphyrin photosensitizers in photodynamic therapy and its applications. *Oncotarget* **8**, 81591 (2017).

41 Vatansever, F. *et al.* Antimicrobial strategies centered around reactive oxygen species–bactericidal antibiotics, photodynamic therapy, and beyond. *FEMS microbiology reviews* **37**, 955-989 (2013).

42 Liu, J., Bin, Y. & Matsuo, M. Magnetic behavior of Zn-doped Fe3O4 nanoparticles estimated in terms of crystal domain size. *The Journal of Physical Chemistry C* **116**, 134-143 (2011).

43 Gupta, R., Sood, A., Metcalf, P. & Honig, J. Raman study of stoichiometric and Zn-doped Fe 3 O 4. *Physical Review B* **65**, 104430 (2002).

44 Wen, M., Li, Q. & Li, Y. Magnetic, electronic and structural properties of ZnxFe3− xO4. *Journal of Electron Spectroscopy and Related Phenomena* **153**, 65-70 (2006).

45 Verde, E. L., Landi, G. T., Gomes, J. d. A., Sousa, M. H. & Bakuzis, A. F. Magnetic hyperthermia investigation of cobalt ferrite nanoparticles: Comparison between experiment, linear response theory, and dynamic hysteresis simulations. *Journal of Applied Physics* **111**, 123902 (2012).

46 Rosensweig, R. E. Heating magnetic fluid with alternating magnetic field. *Journal of magnetism and magnetic materials* **252**, 370-374 (2002).

47 Chaurasia, A. K. *et al.* Coupling of radiofrequency with magnetic nanoparticles treatment as an alternative physical antibacterial strategy against multiple drug resistant bacteria. *Scientific reports* **6** (2016).

48 Li, Y. *et al.* A photoactive porphyrin-based periodic mesoporous organosilica thin film. *Journal of the American Chemical Society* **135**, 18513-18519 (2013).

49 Model, P., and M. Russell. *Filamentous bacteriophage*. Vol. 2 375–456 (Plenum Publishing Corp, 1988).

50 Smith, G. P. Filamentous fusion phage: novel expression vectors that display cloned antigens on the virion surface. *Science* **228**, 1315-1317 (1985).

51 Hengen, P. N. Purification of His-Tag fusion proteins from Escherichia coli. *Trends in biochemical sciences* **20**, 285-286 (1995).

52 Janson, J.-C. *Protein purification: principles, high resolution methods, and applications*. Vol. 151 (John Wiley & Sons, 2012).

53 Bornhorst, J. A. & Falke, J. J. in *Methods in enzymology* Vol. 326 245-254 (Elsevier, 2000).

54 Rai, S. & Manjithaya, R. Fluorescence microscopy: A tool to study autophagy. *AIP Advances* **5**, 084804 (2015).

55 Pickering, A. M. & Davies, K. J. A simple fluorescence labeling method for studies of protein oxidation, protein modification, and proteolysis. *Free Radical Biology and Medicine* **52**, 239-246 (2012).

56 Shepherd, D. *et al.* The process of EDC-NHS cross-linking of reconstituted collagen fibres increases collagen fibrillar order and alignment. *APL materials* **3**, 014902 (2015).

57 Prakash, C. & Vijay, I. K. A new fluorescent tag for labeling of saccharides. *Analytical biochemistry* **128**, 41-46 (1983).

58 Stepanenko, O. V., Verkhusha, V. V., Kuznetsova, I. M., Uversky, V. N. & Turoverov, K. Fluorescent proteins as biomarkers and biosensors: throwing color lights on molecular and cellular processes. *Current Protein and Peptide Science* **9**, 338-369 (2008).

59 Parodi, A. *et al.* Synthetic nanoparticles functionalized with biomimetic leukocyte membranes possess cell-like functions. *Nature nanotechnology* **8**, 61 (2013).

60 Moats, W. A. Kinetics of thermal death of bacteria. *Journal of Bacteriology* **105**, 165-171 (1971).

61 Xie, C., Li, Y.-q., Tang, W. & Newton, R. J. Study of dynamical process of heat denaturation in optically trapped single microorganisms by near-infrared Raman spectroscopy. *Journal of Applied Physics* **94**, 6138-6142 (2003).

62 Carrey, J., Mehdaoui, B. & Respaud, M. Simple models for dynamic hysteresis loop calculations of magnetic single-domain nanoparticles: Application to magnetic hyperthermia optimization. *Journal of Applied Physics* **109**, 083921 (2011).

63 Harmon, B. *et al.* Cell death induced in a murine mastocytoma by 42–47 C heating in vitro: evidence that the form of death changes from apoptosis to necrosis above a critical heat load. *International journal of radiation biology* **58**, 845-858 (1990).

64 Ianzini, M. M., F. Enhancement of radiation-induced mitotic catastrophe by moderate hyperthermia. *International journal of radiation biology* **76**, 273-280 (2000).

65 Sapareto, S. A., Hopwood, L. E., Dewey, W. C., Raju, M. R. & Gray, J. W. Effects of hyperthermia on survival and progression of Chinese hamster ovary cells. *Cancer Research* **38**, 393-400 (1978).

66 VanderWaal, R., Malyapa, R. S., Higashikubo, R. & Roti, J. L. R. A comparison of the modes and kinetics of heat-induced cell killing in HeLa and L5178Y cells. *Radiation research* **148**, 455-462 (1997).

67 Roti Roti, J. L. Cellular responses to hyperthermia (40–46 C): Cell killing and molecular events. *International Journal of hyperthermia* **24**, 3-15 (2008).

68 Stege, G., Li, L., Kampinga, H., Konings, A. & Li, G. Importance of the ATP-binding domain and nucleolar localization domain of HSP72 in the protection of nuclear proteins against heat-induced aggregation. *Experimental cell research* **214**, 279-284 (1994).

69 Kampinga, H., Brunsting, J., Stege, G., Konings, A. & Landry, J. Cells Overexpressing Hsp27 Show Accelerated Recovery from Heat-Induced Nuclear-Protein Aggregation. *Biochemical and biophysical research communications* **204**, 1170-1177 (1994).

70 Lepock, J. R., Frey, H. E., Rodahl, A. M. & Kruuv, J. Thermal analysis of CHL V79 cells using differential scanning calorimetry: implications for hyperthermic cell killing and the heat shock response. *Journal of cellular physiology* **137**, 14-24 (1988).

71 Shah, B. P. *et al.* Core–shell nanoparticle-based peptide therapeutics and combined hyperthermia for enhanced cancer cell apoptosis. *Acs Nano* **8**, 9379-9387 (2014).